Improved Precision Measurement of Refractive Indices of Gases Using Frequency Comb

J. Zhang, Z. H. Lu, and L. J. Wang
Institute of Optics, Information and Photonics
Max-Planck Research Group and University Erlangen-Nuremberg
91058 Erlangen, Germany
zlu@optik.uni-erlangen.de

***Abstract*—We report improved precision measurement of the refractive index of air and CO_2 using a highly unbalanced Mach-Zehnder interferometer with a frequency comb as the light source. The deviation of our experimental results with Edlén's formula is 1.4×10^{-9} at 800 nm. Our experiment has a standard error of 5.2×10^{-9} at fixed parameters (pressure and temperature). The result for CO_2 shows a bigger deviation with earlier results of Old et al. by 4.78×10^{-6} at 800 nm.**

I. INTRODUCTION

The accurate knowledge of the refractive indices of the constituent gases of air is very important in optical metrology, lidar, pollution monitoring, and geodetic surveying. A continuous wave (CW) laser refractometer is traditionally used to measure the refractive indices of gases, and is based on the technique of counting interference fringes of a known optical path, which is alternatively evacuated or filled with gas. The disadvantage of CW laser refractometer is that only limited wavelengths can be measured.

We recently developed a new method of measuring the refractive indices of gases over a broad bandwidth using a femtosecond frequency comb. A multipass cell filled with pure gas is used in one arm of the Mach-Zehnder interferometer, while the other arm, controlled by a stepper motor, acts as the reference path. Both time and frequency domain interferograms are recorded. The time domain signal is used to calculate the length of the multipass cell. The frequency domain signal is used to calculate the phase difference of the interferometer. The knowledge of this phase difference, together with the knowledge of the multipass cell length, enables us to calculate the refractive indices of gases. The multipass cell is used to enhance the resolution of the experiment. Due to the long length of the multipass cell, a phase-locked femtosecond laser is required to ensure clear fringe structure in time domain and phase stability in frequency domain. This phase-locking can be achieved by utilizing the frequency comb technique.

In order to improve the accuracy of our experiment, we put the multipass cell into a temperature-stabilized box, and lock the interferometer's path-length, excluding the cell, with a He-Ne laser. A temperature stabilization of 0.6 mK using a digital PID controller, which corresponds to 0.4 μm multipass cell length change, is reached. The fluctuation of the interferometer path-length is also suppressed to approximately 7 nm with a He-Ne interferometer. Finally, much more accurate, absolute thermometer and pressure gauge are used to measure the temperature and pressure. With these improvements, an uncertainty limit of 7.7×10^{-9} can be achieved. For air measurement, the present result shows a deviation with Edlén's formula of 1.4×10^{-9} at 800 nm with a standard error of 5.2×10^{-9} [1, 2]. For CO_2 measurement, the deviation with Old et al.'s result is 4.78×10^{-6} at 800 nm, with a standard error of 3.3×10^{-9}.

II. EXPERIMENTAL SETUP

The experimental setup is shown in Fig. 1. The light source is a femtosecond, mode-locked, Ti:sapphire laser frequency comb (MenloSystems FC-8004) whose repetition rate and carrier envelope phase are both locked to a Cs frequency standard (Agilent 5071A). The laser has a repetition rate of 200 MHz. The center wavelength is approximately 800 nm, with an original bandwidth of approximately 50 nm. The laser power used is approximately 20 mW. In the experiment the laser beam is divided into two paths using a beamsplitter. The first beam goes through a multipass cell (Toptica CMP-30) that is filled with pure gases. The total path length inside the mutlipass cell is approximately 30 m. The other beam goes through a shorter, adjustable, reference arm. The two beams are recombined at a second beamsplitter with equal intensity, and one of the outputs is sent into a fast photodiode as the time domain signal, analyzed with an Agilent 83480A communications analyzer. The other output is coupled into an Ando AQ6317B optical spectrum analyzer through a short length single-mode fiber as the frequency domain signal. Both the time and frequency domain signals are recorded and processed by a computer.

1-4244-0647-1/07/$20.00 ©2007 IEEE

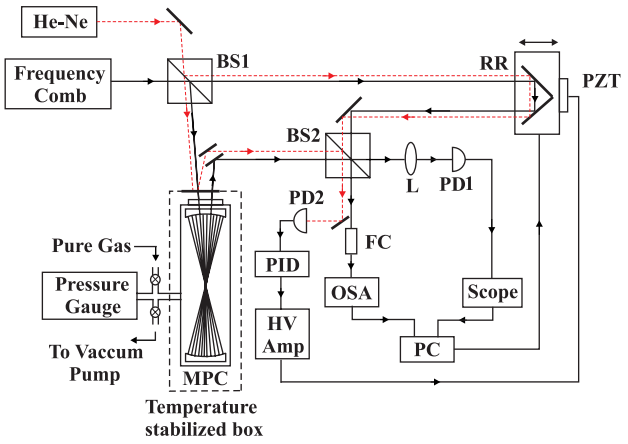

Figure 1. Experimental setup. BS1, BS2, cube beam splitters; MPC, multipass cell; RR, retroreflector; L, lens; PD1 and PD2, photodiodes; FC, fiber coupler; and OSA, optical spectrum analyzer. The red dashed line corresponds to the He–Ne laser optical path.

In order to circumvent the thermal expansion of the multipass cell we place it inside a temperature-stabilized aluminum box. An aperture is placed on one side of the box to allow optical access to the multipass cell. An optical long pass filter that is reflective at 633 nm is glued to this aperture. This filter serves as the reflector for the He-Ne laser that is used to lock the interferometer path-length outside the temperature-stabilized box, and the filter also serves as a partial heat shield for the temperature-stabilized box. Another hole is drilled on the other side of the box to allow passing of the gas line and electrical connections. The whole box is temperature stabilized by a digital PID controller. With the optimized PID control parameters we are able to obtain a settling time of approximately two hours. The rms temperature fluctuation after settlement is calculated to be 0.6 mK for 25 hours. This corresponds to a multipass cell length change of 0.4 μm for a total length of 30 m.

The interferometer path-length change outside the multipass cell is controlled by locking a copropagating He-Ne laser interferometer. The optical path of the He-Ne laser is shown as dashed line in Fig. 1. One arm of the He-Ne beam is reflected from the front surface of the long pass filter, and is recombined with the other He-Ne beam that goes through the retroreflector, at a cube beamsplitter. The interference signal is detected by a photodiode PD2, and is used as the error signal input to a Toptica PID 110 controller. The output of the PID controller is used to control a piezo that is mounted on the adjustable reference arm. After locking we calculate an rms path-length change of 7 nm. The pressure of the multipass cell is measured with a Paroscientific 760-45A pressure gauge (calibrated by the PTB). The uncertainty of the pressure measurement is 2 Pa.

III. EXPERIMENTAL RESULTS

With the multipass cell temperature stabilized, and the interferometer path length locked, both time and frequency domain interference signals can be measured. In the time domain the interference signal has the form

$$I(\tau) \propto \left\langle |E_1(t-\tau)|^2 \right\rangle + \left\langle |E_2(t)|^2 \right\rangle + \left\langle E_1(t-\tau)E^*{}_2(t) \right\rangle + \left\langle E^*{}_1(t-\tau)E_2(t) \right\rangle, \quad (1)$$

in which the angle brackets indicate the time averaging done by the detector and τ is the time delay between the two paths. The time delay can be varied by changing the repetition rate f of the laser. The relationship between the time delay τ and the repetition rate f is

$$\tau = N\delta f / f^2, \quad (2)$$

in which δf is the change of the repetition rate. N is an integer such that the initial pulse from the multipass cell arm overlaps with the (N+1)th pulse from the reference arm, with a time delay of Nc/f. By first overlapping the two pulses at repetition rate f_1, and then moving the stepper motor for a known distance δl, and overlapping the two pulses again at repetition rate f_2, we can calculate the N to be $N=f_1 f_2 \delta l/c(f_1+f_2)$. In our experiment, N is measured to be 20, corresponding to a relative path-length difference of about 30 m.

In the experiment, we first evacuate the multipass cell to vacuum. We adjust the stepper motor so that the pulse from the multipass cell arm almost overlaps with the 20th pulse from the reference arm. The laser repetition rate is then scanned at a 0.4 Hz step size while the laser remains frequency and phase locked. An interferogram is obtained. Then we fill the multipass cell with air or CO_2 to a preset pressure of approximately 10^5 Pa. We then scan the laser repetition rate at a 0.4 Hz step size again to obtain another interferogram. One of the scan results is shown in Fig. 2(a). The repetition rate difference f_1-f_2 from the peaks of the two interferograms is measured, and from Eq. (2) we can calculate the group delay from the multipass cell $\tau_g=N(f_1-f_2)/f_1f_2$. Since

$$\tau_g = \frac{[n_g(\lambda_0)-1]l_{cell}}{c}, \quad (3)$$

we can then calculate the total length of the multipass cell l_{cell}. Here $n_g(\lambda)=n(\lambda)-\lambda dn(\lambda)/d\lambda$ is the group index of the gas, and λ_0=800 nm is the center wavelength of the laser pulse. In a first-order approximation we can directly calculate the group index by using known refractive index formula of different gases, from which we can obtain l_{cell}. The uncertainty of l_{cell} is approximately 0.9 mm. This uncertainty is mainly due to the uncertainty of the refractive index formula. The effect of the multipass cell length change due to evacuation has been investigated before [3], and we estimate it to be less than 6 nm in our case.

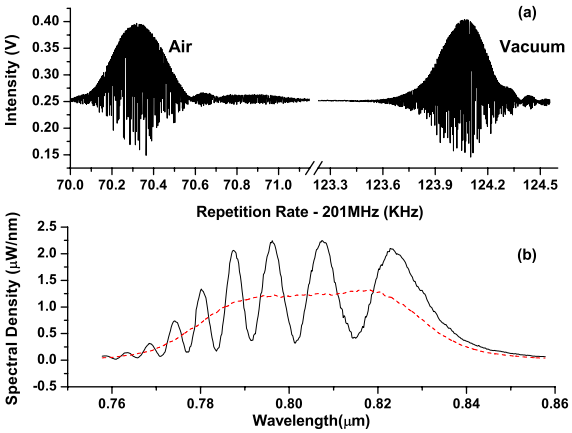

Figure 2. (a) Interferograms in the time domain vs laser repetition rate when the multipass cell is filled with standard air or pumped out to vacuum. (b) Interferograms in the frequency domain. The solid curve shows spectral modulation, and the dotted curve shows no spectrum interference.

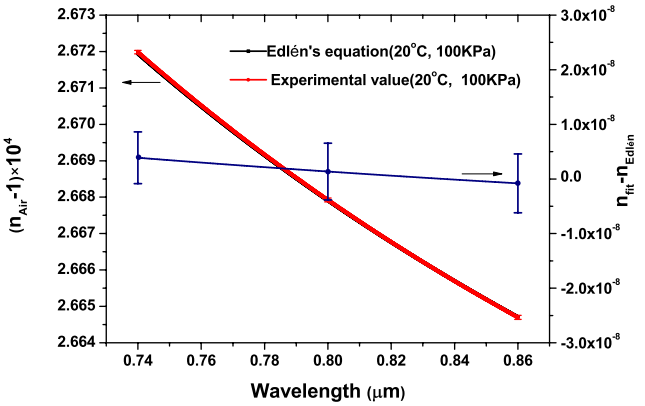

Figure 3. (Left panel) Nonlinear least-squares fitting of the measured refractive index of air. (Right panel) Difference between the fitted result and Edlén's formula. The standard error of the 800 nm data point is 5.2×10^{-9}.

Frequency domain interferograms are simultaneously taken to obtain the refractive index. In the frequency domain we are dealing with the phase delay, and the interference signal has the form

$$I(\omega) = I_1(\omega) + I_2(\omega) + 2\sqrt{I_1 I_2}\cos\Phi(\omega), \qquad (4)$$

where $I_1(\omega)$ and $I_2(\omega)$ represent the spectral densities of the two interfering beams. A spectral modulation will be observed at the output of the optical spectrum analyzer when the two arms are unbalanced. The modulation period is inversely proportional to the delay of the two arms. When the delay is too large (the maximum time delay we can achieve with a 200 MHz laser is 2.5 ns), such that the period is much smaller than the optical spectrum analyzer's resolution, the spectral modulation will be washed out, and we get only $I_1(\omega)+I_2(\omega)$. This result is shown in Fig. 2(b), where the solid curve corresponds to spectral modulation $I(\omega)$, and the dotted curve corresponds to no spectral modulation $I_1(\omega)+ I_2(\omega)$. The phase $\Phi(\omega)$ can be measured with the same technique used by Dogariu et al. [4].

When the multipass cell is filled with pure gas, the phase,

$$\Phi_{gas}(\omega) = \frac{\omega(nl_{cell} + n'\Delta l)}{c} + \phi'(\omega), \qquad (5)$$

can be measured. Here n' is the refractive index of air outside the multipass cell, Δl is the path-length difference of the two arms excluding the contributions from the multipass cell and cell window. $\phi(\omega)$ represents a common phase shift including those introduced by the window and the multi-reflecting mirrors. Similarly, when the multipass cell is pumped to vacuum, the phase,

$$\Phi_{vac}(\omega) = \frac{\omega(l_{cell} + n'\Delta l)}{c} + \phi'(\omega), \qquad (6)$$

is also measured. From (5) and (6) we can calculate the phase difference

$$\Delta\Phi(\omega) = \Phi_{gas}(\omega) - \Phi_{vac}(\omega) = \frac{(n-1)l_{cell}\omega}{c}. \qquad (7)$$

From Eq. (7) we can then calculate the refractive indices of different gases to be

$$n_{gas}(\lambda) = 1 + \frac{\lambda\Delta\Phi}{2\pi l_{cell}}. \qquad (8)$$

For air measurement, with the relative uncertainties associated with $\lambda(1.9\times10^{-5})$, $\Delta\Phi$ (9.2×10^{-6}), and $l_{\rm cell}$ (3.0×10^{-5}), we can estimate that our experiment has a sensitivity of 9.6×10^{-9}. We took 40 measurements with pressures close to 1 bar. The results are first converted into standard dry air conditions (20°C, 1 bar, 400 ppm CO_2) [5]. The average is then least-squares fitted with the standard formula $(n\text{-}1)\times10^8 = A_0 + A_1/(B_1\text{-}1/\lambda^2) + A_2/(B_2\text{-}1/\lambda^2)$ [6]. The fitted parameters are

$$A_0=7799.462,\ A_1=2339307,\ A_2=20197.51,$$

$$B_1=128.0630,\ B_2=53.70979.$$

The result is compared with Edlén's formula, and shown in Fig. 3. As can be seen, our result is very close to that of Edlén's formula. At the wavelength of 800 nm, our measured refractive index of air is $n_{\rm fit}$=1.0002667925(52), compared with Edlén's result of $n_{\rm Edlén}$=1.0002667911, the difference is 1.4×10^{-9} with a standard error of 5.2×10^{-9}.

It is very important to measure the CO_2 contribution to the air refractive index. For CO_2 measurement, our experiment has a sensitivity of 1.6×10^{-8}, taking into account of the relative uncertainties of $\lambda(1.9\times10^{-5})$, $\Delta\Phi$ (5.6×10^{-6}), and $l_{\rm cell}$ (3.0×10^{-5}). We took 20 measurements with pressures close to 1 bar. The results are converted into 1 atm and 0 °C conditions in order to compare with Old et al.'s result [7], which has an uncertainty of 6.0×10^{-7}. The fitting formula we used is $(n\text{-}1)\times10^8 = A_0 +$

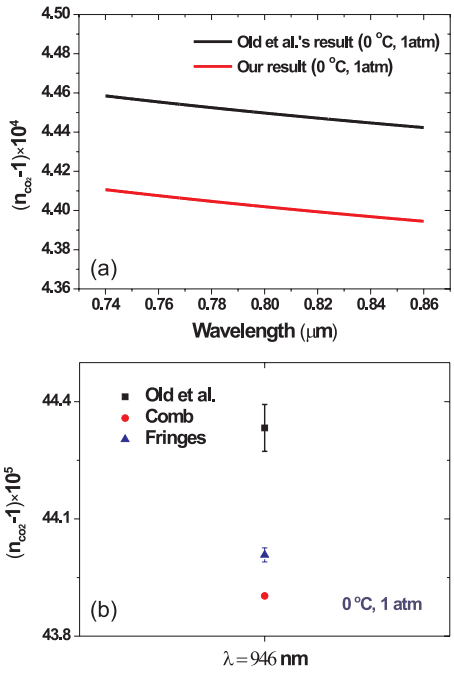

Figure 4. (a) Wavelength dependence of the refractive index of CO_2. The red curve is our result, and the black curve is from Old et al. (b) The refractive index of CO_2 at 946nm, obtained by different methods.

$A_1/(B_1\text{-}1/\lambda^2) + A_2/(B_2\text{-}1/\lambda^2) + A_3/(B_3\text{-}1/\lambda^2)$. The fitted parameters are

$$A_0 = -1296.236,$$

$$A_1 = 173.4113,\ A_2 = 313565.5,\ A_3 = 8362226,$$

$$B_1 = 0.0584738,\ B_2 = 71.86301,\ B_3 = 205.6656.$$

The difference with Old et al.'s result, shown in Fig. 4(a), is 4.78×10^{-6} at 800 nm with standard error of 3.3×10^{-9}. We notice that a wrong density factor formula was used when they converted their measurement results to standard conditions. Since Old et al.'s paper did not give the exact experimental conditions under which they took their data, we cannot be absolutely sure about the real difference. To investigate the causes of this discrepancy, we performed a CW laser refractometer fringe counting experiment. The experiment setup is very similar to Fig. 1, except we use an ultra-stable Nd:YAG laser at 946 nm (< 1 kHz at 1 sec) as the light source, and count the total number of interference fringe when the multipass cell is slowly filled with gas. We take two measurements, one with the multipass cell slowly filled with dry air from vacuum, and the other with the multipass cell slowly filled with CO_2 from vacuum, and by taking the air refractive index as the reference, we can calculate the refractive index of CO_2 at 946 nm. The result is shown in Fig. 4(b). The fringe counting experiment has a smaller deviation with the frequency comb experimental result. The uncertainty of the fringe counting experiment is worse than the frequency comb experiment due to environmental disturbances. Improvement of this technique is on-going.

IV. CONCLUSION

In conclusion, we demonstrate a method of measuring the refractive index of air and CO_2 using a frequency comb. A sensitivity of 9.6×10^{-9} is demonstrated for air measurement. Our result agrees with that of Edlén's formula at 800 nm to within 1.4×10^{-9} with a standard error of 5.2×10^{-9}. This accuracy level is reached by sub-mK absolute temperature measurement and stabilization of the multipass cell by locking the interferometer path-length. In addition, we measure the absolute pressure to an accuracy of 2 Pa. Taking into account of the accuracy of temperature and pressure measurement, an uncertainty limit of 7.7×10^{-9} can be achieved.

For CO_2 measurement, our result shows a greater difference with Old et al.'s result. The difference is 4.78×10^{-6} at 800 nm, with a standard error of 3.3×10^{-9}. The experimental sensitivity is 1.6×10^{-8}. We are still investigating the sources of this discrepancy.

In the future, we would like to perform more refractive index measurement of the constituent gases of air, such as O_2, N_2, and Ar. It is hope that with the better resolution and accuracy associated with this experimental technique, we can test the Lorenz-Lorentz equation with much higher accuracy.

ACKNOWLEDGMENT

We thank W. Sabuga of PTB for helpful discussion and the loan of a calibrated Paroscientific pressure gauge.

REFERENCES

[1] J. Zhang, Z. H. Lu, and L. J. Wang, "Precision measurement of the refractive index of air with frequency combs," Opt. Lett., vol. 30, pp. 3314-3316, 2005.

[2] J. Zhang, Z. H. Lu, B. Menegozzi, and L. J. Wang, "Application of frequency combs in the measurement of the refractive index of air," Rev. Sci. Instrum., vol. 77, p. 083104, 2006.

[3] K. P. Birch, M. J. Downs, and D. H. Ferriss, "Optical path length changes induced in cell windows and solid etalons by evacuation," J. Phys. E, vol. 21, pp. 690-692, 1988.

[4] A. Dogariu, A. Nahata, R. A. Linke, L. J. Wang, and R. Trebino, "Optical pulse propagation through metallic nano-apertures," Appl. Phys. B, vol. 74, pp. S69-S73, 2002.

[5] G. Bönsch and E. Potulski, "Measurement of the refractive index of air and comparison with modified Edlén's formulae," Metrologia, vol. 35, pp. 133-139, 1998.

[6] B. Edlén, "The Refractive Index of Air," Metrologia, vol. 25, pp. 71-80, 1966.

[7] J. G. Old, K. Gentill, and E. R. Peck, "Dispersion of Carbon Dioxide," J. Opt. Soc. Am., vol. 61, p.89, 1971.